Self-assembly of porphyrin–azulene–porphyrin and porphyrin–azulene conjugates†

Ze-Yun Xiao, Xin Zhao,* Xi-Kui Jiang and Zhan-Ting Li*

Received 26th February 2009, Accepted 1st April 2009
First published as an Advance Article on the web 28th April 2009
DOI: 10.1039/b904009a

In this paper we report the synthesis and self-assembling behavior of new porphyrin-azulene-porphyrin and porphyrin-azulene conjugates. The porphyrin-azulene-porphyrin conjugate gelates a number of organic solvents, while the porphyrin-azulene conjugates form vesicles in a chloroform–methanol binary mixture. The structures of the organogels and vesicles have been characterized by SEM and AFM. Two porphyrin-naphthalene-porphyrin and porphyrin-naphthalene conjugates were also prepared. A comparison of their properties with those of the azulene analogues reveals that the intermolecular dipole–dipole interaction of the azulene units plays an important role in promoting the self-assembly of the porphyrin-azulene-porphyrin and porphyrin-azulene conjugates.

Introduction

Supramolecular self-assembly of large π-conjugated systems is an exciting research area due to their potential applications in advanced electronics and photonics. In this context, conjugated porphyrin has attracted special attention because of its unique photophysical and photochemical properties.[1] At present, a large number of supramolecular systems, such as nano fibers and tubes,[2–6] vesicles,[7,8] interlocked topological architectures[9–11] and organogels,[12–16] have been constructed based on various porphyrin derivatives. An effective strategy of creating porphyrin supramolecular systems is to introduce new tunable functional groups. In such a way, a specific assembling property may be remarkably tuned or improved.

Azulene is a polar structural isomer of naphthalene that consists of a five-membered ring fused to a seven-membered ring (Fig. 1). It has a permanent dipole moment of 1.08 D and an aromatic stabilization energy that is nearly 5 times lower than that of benzene,[17,18] which gives it some unusual characteristics such as remarkably low HOMO–LUMO separation.[19,20] In recent years, azulene derivatives have been applied in developing discrete advanced materials including nonlinear chromophores,[21] liquid crystals,[22] organic semiconductors,[23] conducting polymers[24] and charge-transfer complexes.[25,26] Although the synthesis of a few porphyrin-azulene conjugates have been reported,[27,28] their assembling behavior has not been described yet. We herein report the synthesis of three new porphyrin-azulene-porphyrin and porphyrin-azulene conjugates and their formation of organogels and vesicles which are enhanced by the dipole–dipole interaction of the azulene units.

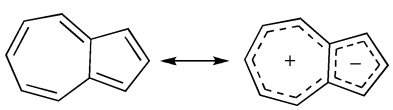

Fig. 1 Azulene and its resonance form which characterizes its polar nature.

State Key Lab of Bioorganic and Natural Products Chemistry, Shanghai Institute of Organic Chemistry, Chinese Academy of Sciences, 345 Lingling Lu, Shanghai, 200032, China. E-mail: xzhao@mail.sioc.ac.cn, ztli@mail.sioc.ac.cn; Fax: 0086-21-64166128; Tel: 0086-21-54925122

† Electronic supplementary information (ESI) available: NMR and IR spectra of compounds **5**, **6** and **T1–T5**. See DOI: 10.1039/b904009a

Results and discussion

Synthesis

Compounds **T1–T3** were designed and synthesized.

For the investigation of the effect of the azulene unit on the self-assembling property, naphthalene derivatives **T4** and **T5**, the isomers of **T1** and **T3**, were also prepared. The synthetic routes are provided in Scheme 1. Thus, compound **1**[29] was first selectively hydrolyzed with barium hydroxide to afford **2**. The acid was then coupled with porphyrin **3**[30] to generate **T2** in 67% yield. After treatment with formic acid in dichloromethane, **T2** was further converted to the corresponding acid, which was then coupled with **3** to give **T1** in 67% yield. For the preparation of **T3**, **1** was first treated with formic acid to form the corresponding acid, which was then coupled with **3** to afford **T3** in 74% yield. For the synthesis of **T4**, diacid **4** was first converted to the corresponding diacyl chloride, which was then treated with **3** to give **T4** in 61% yield. For the preparation of **T5**, diester **5** was first prepared from **4** and then hydrolyzed with lithium hydroxide to give acid **6**, which was then coupled with **3** to afford **T5** in 49% yield.

Gelation test

The gelation properties of **T1–T5** have been tested for twelve organic solvents and the results are shown in Table 1. It can be found that **T1** has the best gelating ability. Among the twelve solvents tested, it can gelate eight solvents. In addition, its lowest gelation concentration is generally lower than the related one of **T4**. The gelating ability of the compounds should be controlled mainly by the intermolecular hydrogen bonding and stacking

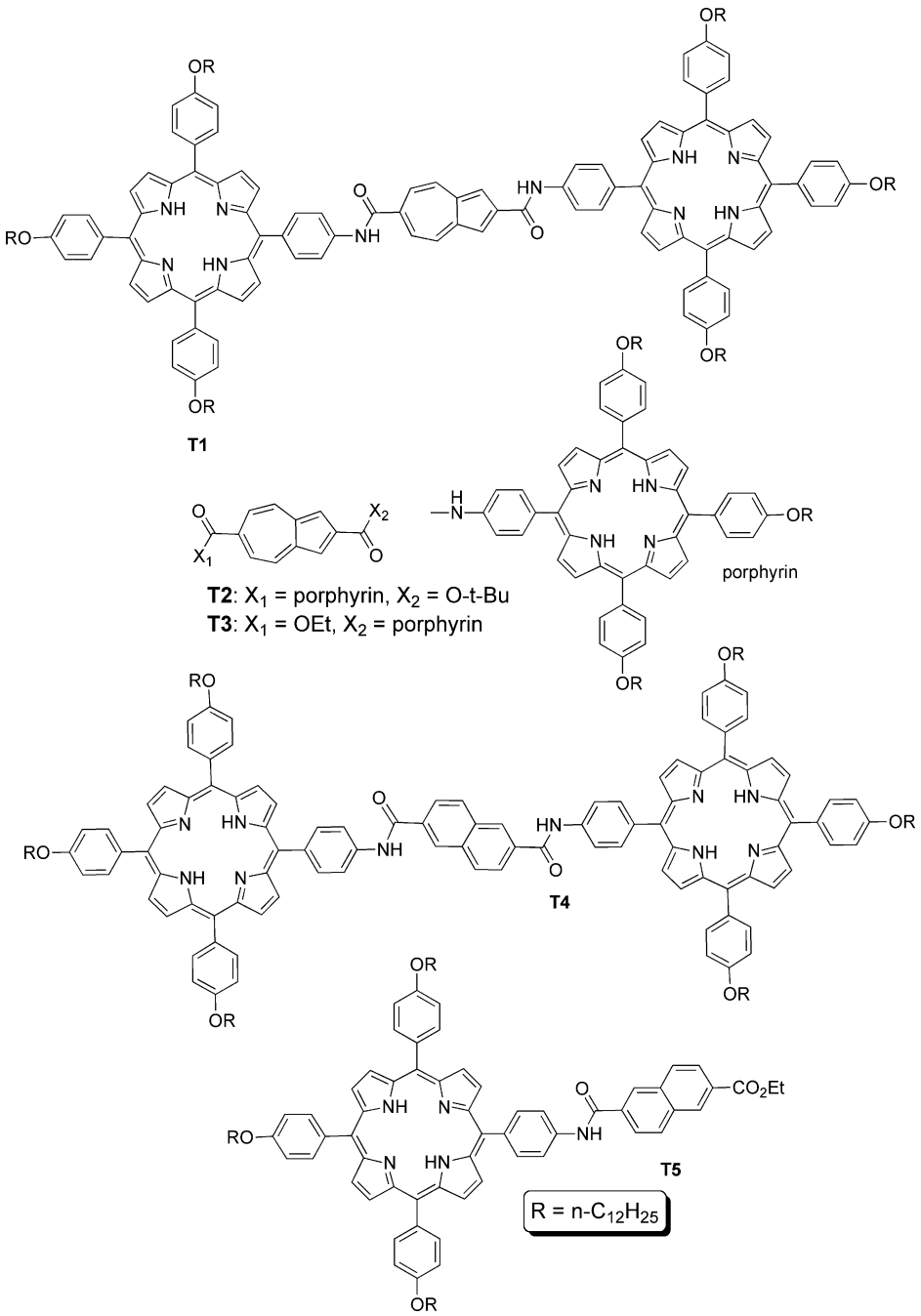

interaction, which induced the formation of three-dimensional networks of fibrous aggregates (Fig. 2, *vide infra*). Considering the similarity of the two compounds, it is reasonable to assume that the intermolecular N—H $\cdots$ O=C hydrogen bonding of their two amides should be comparable in stability. Therefore, the larger gelating ability of **T1** should be attributed to the enhanced stacking of the azulene unit due to its large dipole–dipole interaction,[31] which was particularly important in polar solvents like *n*-octanol, ethyl acetate and DMF, where the intermolecular hydrogen bonding was weakened or destroyed and thus **T4** lost the gelating ability. **T2** and **T3** only gelated *n*-docane partially, although **T3** also gelated cyclohexane, implying that the stacking interaction of the porphyrin unit also played an important role in gelating the solvents. This result also supported the importance of the dipole–dipole interaction of the azulene unit, because this interaction required that the azulene unit stacked alternately, which would force the porphyrin units of **T2** and **T3** to orientate oppositely. **T5** did not gelate any solvents, further setting off the promoting effect of the azulene unit.

Morphology studies

The morphology of the resulting gels was characterized by SEM. SEM images of the *trans*-decalin xerogels of **T1** and **T4** displayed entangled fibrils of micrometres in length and hundreds of nanometres in width, which is characteristic of a gel state

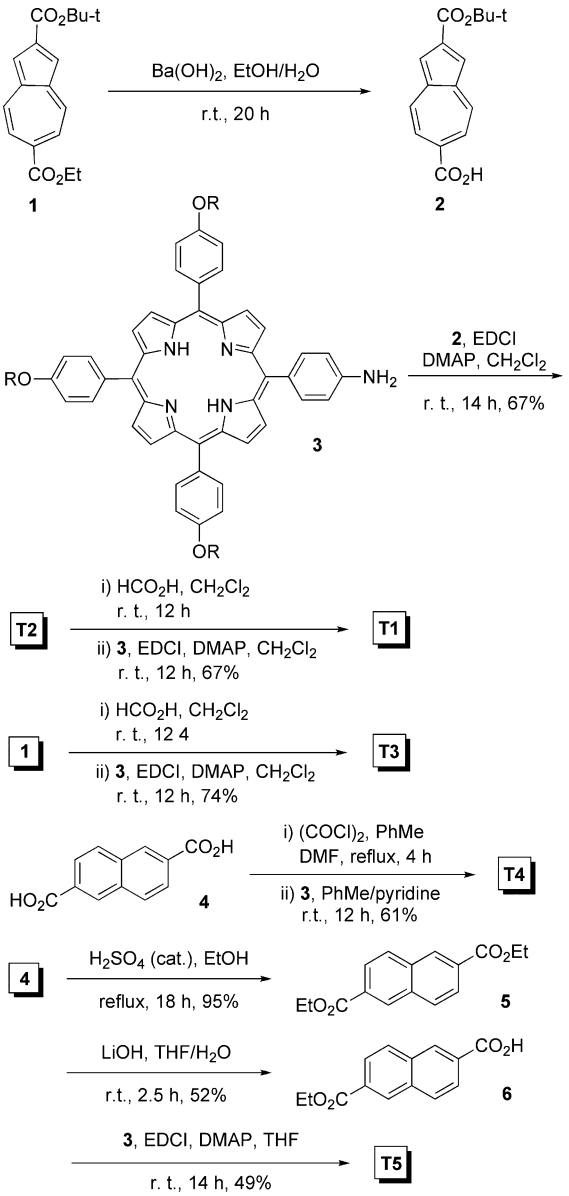

Scheme 1 The synthetic routes to compounds **T1–T5**.

(Fig. 2a and 2b). AFM images of the solution sample of **T1** in cyclohexane (0.1 mM) also gave rise to networks of nanofibrils (Fig. 2c). If the evaporating process went quickly, only shorter nanowires were generated (Fig. 2d). These results supported a slow 1D stacking process for the formation of the fibrous structures.[32]

The formation of nanofibrils by **T1** was also supported by the SEM image (Fig. 2e). **T4** at the same low concentration also self-assembled into wirelike structures, however, they were less uniform in width (Fig. 2f), possibly indicating a lower assembling ability.

Fibrous structures were not observed for **T2** and **T3** at low concentrations. However, they were found to self-assemble into vesicular aggregates in the methanol–chloroform binary mixtures when the content of methanol was 20–43%. The samples were insoluble when the content of methanol was further increased. SEM images evidenced the formation of the vesicular structures. The representative images are shown in Fig. 3a and 3b. The

Table 1 Gelation properties of compounds **T1–T4** [a,b]

Solvent	T1	T2	T3	T4
n-Hexane	G (15)	P	P	G (20)
Cyclohexane	G (8)	S	G (20)	G (15)
n-Decane	G (18)	*p*G	*p*G	G (20)
Decalin (*cis*)	G (7)	S	S	G (10)
Decalin (*trans*)	G (5)	S	S	G (8)
Toluene	S	S	S	S
Dichloromethane	S	S	S	S
THF	S	S	S	S
Acetone	S	S	S	S
n-Octanol	G (20)	P	P	P
Ethyl acetate	G (15)	P	P	P
DMF	G (10)	P	P	P

[a] G, P, *p*G and S denote gelation, precipitation, part gelation and solution, respectively. [b] The critical gelation concentration (mM) is showed in parenthesis.

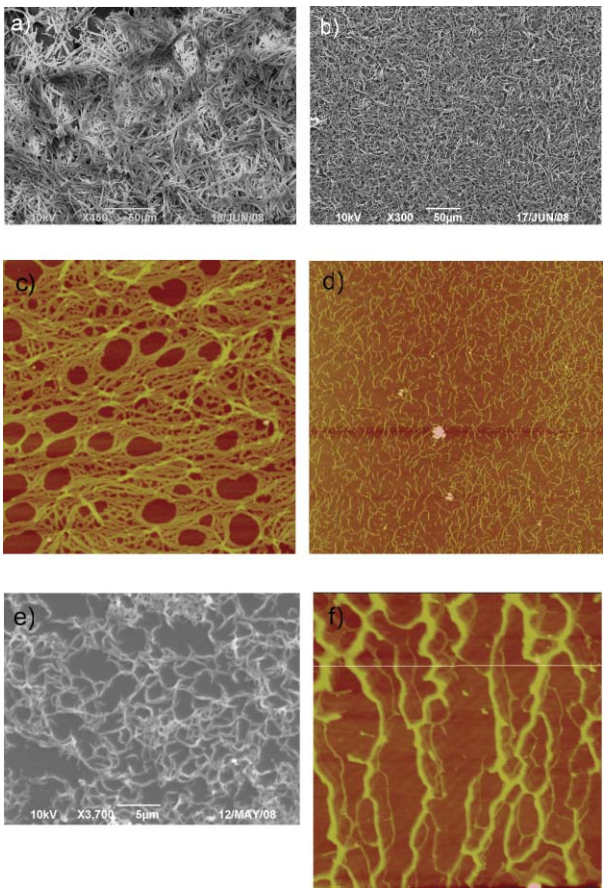

Fig. 2 SEM images of (a) xerogel of **T1** + *trans*-decalin, (b) xerogel of **T4** + *trans*-decalin and (e) **T1** from a 2.0 mM methanol–chloroform (1 : 2) solution and AFM images of **T1** (c) slow evaporation, (d) quick evaporation from a 0.1 mM cyclohexane solution, and (f) **T4** from a 0.1 mM cyclohexane solution. The scan size of AFM is 5 μm × 5 μm.

vesicular structures were also observed on the AFM images (Fig. 3c and 3d). Cross-section analysis of the typical structures revealed a large diameter–height ratio (*ca.* 18.1 and 18.2, respectively), which indicated that they were of flattened shape.[33] The results also supported that the spherical structures were hollow

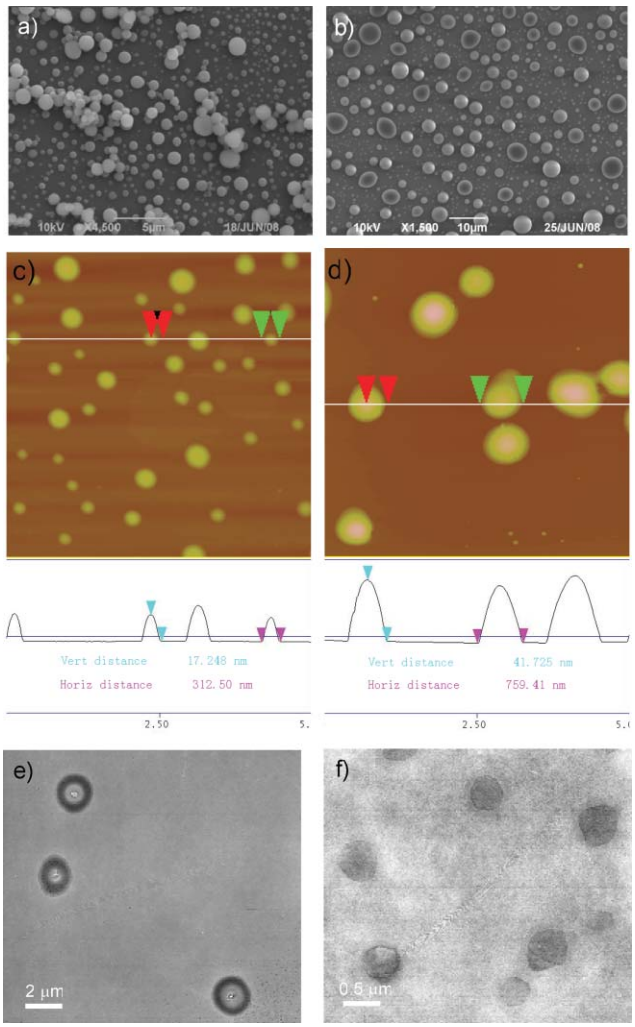

Fig. 3 SEM images of (a) **T2**, (b) **T3** and AFM images and cross-section analysis (bottom ones) of (c) **T2** and (d) **T3** and TEM images of (e) **T2** and (f) **T3**, all obtained from methanol–chloroform (1 : 2). The scan size of AFM is 5 μm × 5 μm.

and contained solvent molecules, which were evaporated after being transferred from the solution to the surface.[34] TEM was also used to investigate the resulting aggregates, and the clear contrast between the peripheral and central areas of the spherical aggregates provided further evidence of their vesicular nature (Fig. 3e and 3f). Under the same conditions, **T5** did not form similar vesicular structures in the methanol–chloroform binary mixtures containing 20% and 43% methanol respectively. The spherical aggregates were observed in the sample of **T5** when the content of methanol was 33%. The result suggested that **T5** had a lower self-assembling ability and proved that the azulene unit in **T2** and **T3** promoted their ordered aggregation. A thermal stability test on the spheres formed by **T3** and **T5** in methanol (33%)–chloroform showed that the vesicles of **T5** collapsed through fusion at 50 °C and were totally destroyed at 60 °C, while the spherical structures of **T3** were still maintained after being heated at 60 °C for 10 minutes (Fig. 4), also suggesting that the dipole–dipole interaction of azulene really makes a contribution to stabilize the resulting self-assembling structures.

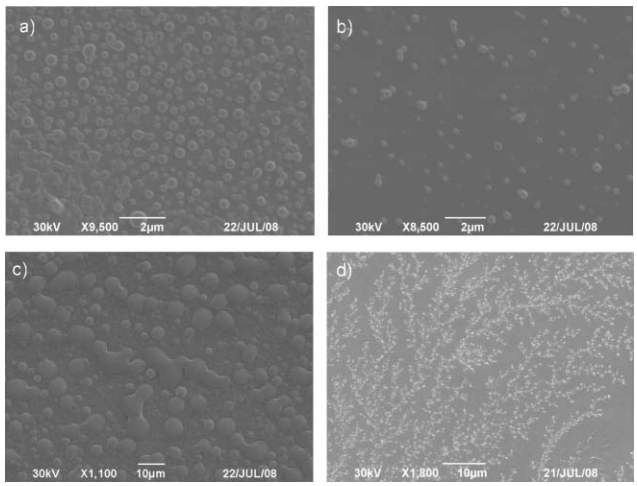

Fig. 4 SEM images of **T3** after incubation at (a) 50 °C and (b) 60 °C and SEM images of **T5** after incubation at (c) 50 °C and (d) 60 °C.

X-Ray diffraction (XRD)

Powder XRD measurements were carried out for the cyclohexane gels of **T1** and **T4**. The profiles are shown in Fig. 5. The gel of **T1** gave rise to four peaks at 31.1, 15.2, 10.8 and 9.2 Å, respectively. Since the extended molecular length of **T1** was estimated to be *ca.* 7.3 nm by CPK modeling (4.7 nm for the skeleton of porphyrins and azulenic unit, and 1.3 nm for each *n*-dodecyl group) and it is reasonable to assume that the *n*-dodecyl groups did not fully extend, the first peak might be assigned to half of the head-to-tail distance between the two adjacent molecules at the longitudinal direction (200 plane), and the second and third peaks should be those of the secondary (400 plane) and third (600 plane) diffractions of the first peak, while the 9.2 Å peak might belong to the edge-to-edge distance of the adjacent molecules. The gel of **T4** displayed a more complicated XRD pattern. Peaks of 24.2, 12.0 and 7.9 Å were observed, besides those at 27.3 (200 plane), 13.6 (400 plane) and 9.0 Å (600 plane), suggesting that order arrangement also existed along another direction besides the one-dimensional growth. The difference shows that **T1** grew into more ordered one-dimensional structures, as revealed by AFM (Fig. 2).

UV-Vis and fluorescence spectroscopies

UV-Vis spectra were recorded for **T1–T4** to investigate their stacking properties. The absorption maximum of the Soret band of **T1** in the cyclohexane solution appeared at 421 nm. However, its UV-Vis spectrum in the cyclohexane gel exhibited two distinct Soret bands, with one red-shifting by 17 nm and another blue-shifting by 9 nm (Fig. 6a). Since the red-shifted Soret band corresponds to a J-type aggregation and the blue-shifting reflects a H-type aggregation,[35] the result suggested that both J- and H-aggregates contributed to the formation of the organogels.[36] The absorption spectrum of the cyclohexane gel of **T4** exhibited a similar red-shift feature (15 nm), together with a small shoulder around 412 nm (Fig. 6b), which suggested that the J-aggregation overwhelmed the H-aggregation. The UV-Vis spectra of **T1–T4** were also recorded in the film state. The films were produced

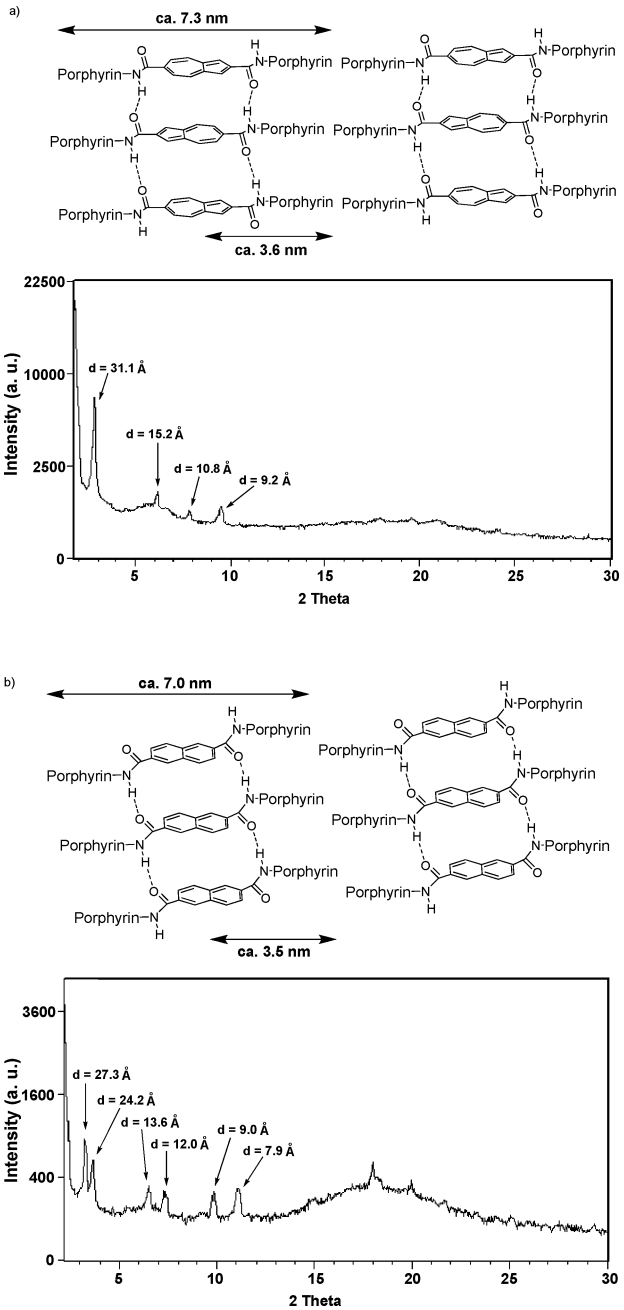

Fig. 5 The schematic images of molecular orientation and powder XRD patterns of the xerogels of (a) **T1** and (b) **T4** obtained from cyclohexane.

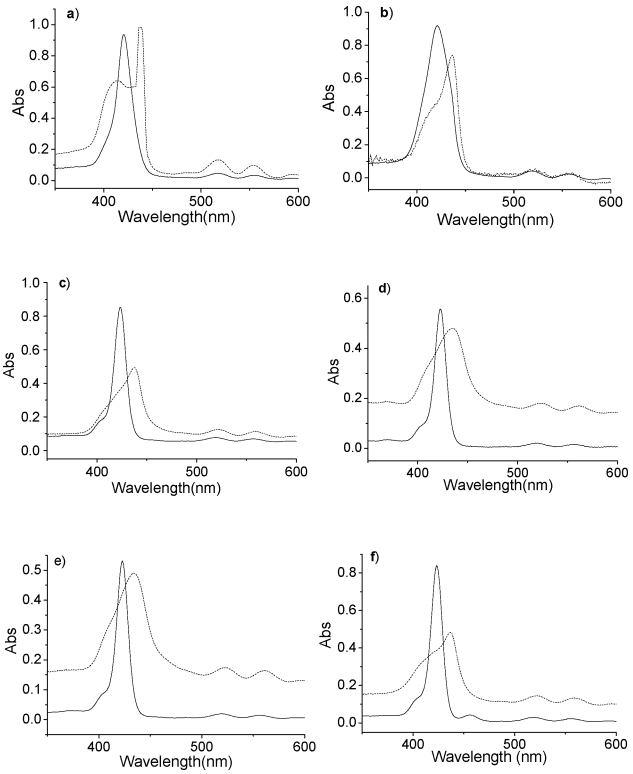

Fig. 6 UV-Vis spectra of (a) **T1** and (b) **T4** in the cyclohexane solution (solid line, 2 μM) and gel (dotted line), (c) **T1** in solution (solid line) and in film state (dotted line), (d) **T2** in solution (solid line) and in film state (dotted line), (e) **T3** in solution (solid line) and in film state (dotted line), and (f) **T4** in solution (solid line) and in film state (dotted line).

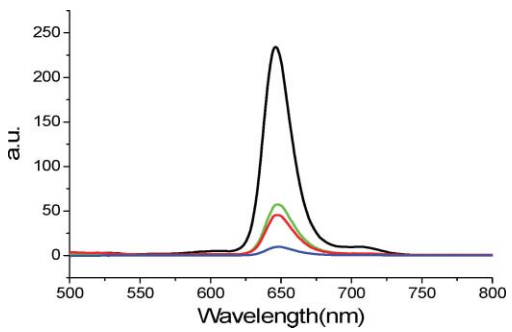

Fig. 7 Fluorescent spectra of **T1** (blue), **T2** (red), **T3** (green) and **T4** (black) in cyclohexane (1.0 μM, excitation wavelength = 423 nm).

by drop-casting their chloroform solution (1.0 mM) on quartz plates. Fig. 6c–6f show their UV-Vis spectra in the film state and in chloroform (1.0 μM). Compared to that (λ_{max} = 423 nm) in the monomeric state in solution, their Soret band in the film state red-shifted by 15 nm, 11 nm, 12 nm, and 14 nm, respectively, indicating that the J-aggregation mode also dominated in the films. **T1** exhibited the largest red-shifting, implying that it possessed the largest J-aggregation. Fluorescent experiments in cyclohexane revealed that, compared to the naphthalene unit in **T4**, the azulenic unit in **T1** remarkably quenched the emission of their porphyrin unit (Fig. 7),[27,28] which was much more effective than that observed for **T2** and **T3**. The result supported that **T1** possessed an increased aggregating tendency, which facilitated the quenching process. Such an increase should be ascribed to the efficient alternate stacking of its azulene unit.

It is well-known that the amide units form intermolecular hydrogen bonding in less polar solvents and this interaction can occur in the presence of polar solvents, such as methanol, when the amide units are shielded by extensive stacking of adjacent segments from competitive solvent molecules, as exhibited by DNA or synthetic systems.[37] As expected, IR studies on dry samples of **T1–T4** after solvent was removed, exhibited NH stretching vibrations only around 3315 cm^{-1} (ESI Fig. S7–10),† indicating that NH units formed intermolecular H-bonding. Therefore, it is reasonable to

propose that the self-assembly process for the azulene-porphyrin conjugates was driven by the cooperation of the hydrogen bonding, porphyrin-porphyrin π-stacking, and dipole–dipole interactions of azulenic units. The strong dipole–dipole interaction dictates the orientation of the array of the molecules to lead to an alternating head-to-tail stacking of the azulene parts for **T1** and **T2** (Fig. 8) and therefore promotes their self-assembling ability.

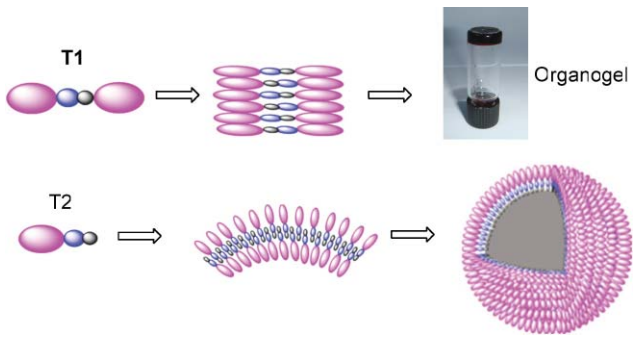

Fig. 8 Proposed mode for the formation of nanowire from **T1** and vesicles from **T2**.

Conclusions

In summary, azulene has been designed to connect to porphyrin to generate a novel type of large π-conjugated structures. The new compounds can self-assemble into one-dimensional aggregates, further entangle into three-dimensional network structures in solution to form organogels, or self-assemble into vesicular structures, depending on the number of porphyrin units in the molecules. The intermolecular dipole–dipole interaction between the azulenic units plays an important role, not only enhancing the self-assembling abilities, but also dictating the orientation in the alignment of the conjugates. In the future, we will try to introduce hydrophilic chains to study their assembling behavior in polar or aqueous media.

Experimental section

General methods

All the reactions were carried out under nitrogen. The ^{1}H NMR spectra were recorded on 300 or 400 MHz spectrometers (Brucker AM-300 or 400) in the indicated solvents. Chemical shifts are expressed in parts per million (δ) using residual solvent protons as internal standards. MALDI-TOF MS were obtained on a Voyager-DE STR or IonSpec4.7 Tesla FTMS spectrometer (CHCA or DHB as matrix). UV-Vis spectra were recorded on a CARY 100 spectrometer, and for the absorption of gels measurements, two quartz plates were used to sandwich a thin layer of the samples. SEM images were obtained with a JEOL model JSM-6390LV and the dry samples obtained were shielded with Pt. AFM pictures were obtained in "tapping" mode on a multimode SPM system equipped with a Nanoscope IV controller. Powder XRD spectra were obtained on a X'Pert PROX system using monochromated Cu Kα (λ = 0.1542 nm) radiation. The transmission electron microscopy (TEM) images were recorded on a JEOL JEM-1230 microscope.

Compound T2

To a stirred saturated solution of barium hydroxide in ethanol and water (1 : 1, 6 mL) was added compound **1** (16 mg, 0.053 mmol) and the solution was stirred at room temperature for 20 h. Diluted hydrochloric acid (1 N) was added to pH = 5 and the solution was concentrated with a rotavapor to *ca.* 3 mL and then extracted with ethyl acetate (10 mL). The organic phase was washed with water (10 mL) and brine (10 mL) and dried over magnesium sulfate. Upon removal of the solvent with a rotavapor, compound **2** was obtained as a green solid, which was then added to a stirred solution of porphyrin **2** (62 mg, 0.052 mmol) and DMAP (10 mg) in CH_2Cl_2 (6 mL). After stirring for 30 min, EDCI (1-ethyl-3-(3-dimethylaminopropyl)carbodiimide hydrochloride) (100 mg, 0.52 mmol) was added to the solution. Stirring was continued for 14 h. Then the mixture was successively washed with water (50 mL), saturated sodium bicarbonate solution (50 mL) and brine (50 mL) and dried over sodium sulfate. After removal of the solvent under reduced pressure, the resulting residue was purified by column chromatography on silica gel (CH_2Cl_2–CH_3OH 100 : 1) to give compound **T2** as a purple solid (50 mg, 67%). ^{1}H NMR (300 MHz, $CDCl_3$): 8.86–8.84 (m, 8 H), 8.44 (s, 1 H), 8.33 (d, J = 10.5 Hz, 2 H), 8.17 (d, J = 8.1 Hz, 2 H), 8.09–7.96 (m, 8 H), 7.70 (s, 2 H), 7.59 (d, J = 10.5 Hz, 2 H), 7.24–7.16 (m, 6 H), 4.18–4.13 (m, 6 H), 1.96–1.91 (m, 6 H), 1.69 (s, 9 H), 1.59–1.53 (m, 6 H), 1.47–1.25 (m, 48 H), 0.92–0.87 (m, 9 H), –2.73 (s, 2 H). ^{13}C NMR (300 MHz, $CDCl_3$): 168.7, 165.0, 159.0, 158.9, 145.6, 142.4, 140.2, 139.3, 138.9, 137.7, 135.7, 135.6, 135.2, 135.1, 134.4, 134.3, 131.3, 131.2, 130.8, 121.8, 120.2, 120.1, 120.0, 119.0, 118.5, 112.9, 112.8, 112.7, 81.5, 68.3, 32.0, 30.3, 29.8, 29.7, 29.6, 29.5, 29.4, 29.3, 28.4, 26.3, 22.8, 14.2. MS (MALDI-TOF): m/z 1437 $[M + H]^+$. HRMS (MALDI-TOF): Calcd. for $C_{96}H_{118}N_5O_6$: 1436.9077. Found: 1436.9089.

Compound T1

A solution of **T2** (55 mg, 0.038 mmol) in formic acid (3 mL) and CH_2Cl_2 (4 mL) was stirred at room temperature for 12 h and concentrated to give the corresponding acid, which was then added to a stirred solution of **3** (45 mg, 0.038 mmol) and DMAP (20 mg) in CH_2Cl_2 (10 mL). After EDCI (100 mg, 0.52 mmol) was added, the mixture was stirred at room temperature for 12 h and then worked up as described above for **T2**. The crude product was purified by column chromatography (twice) on silica gel (CH_2Cl_2–THF 100 : 1) to give **T1** as a purple solid (65 mg, 67%). ^{1}H NMR (300 MHz, THF-d_8): 9.06–8.98 (m, 16 H), 8.83 (d, J = 10.5 Hz, 2 H), 8.48 (d, J = 8.4 Hz, 2 H), 8.40–8.34 (m, 6 H), 8.24–8.16 (m, 14 H), 8.01 (d, J = 10.5 Hz, 2 H), 7.45–7.37 (m, 12 H), 4.40–4.34 (m, 12 H), 2.09–2.07 (m, 12 H), 1.78–1.76 (m, 12 H), 1.63–1.45 (m, 96 H), 1.15–1.00 (m, 18 H), –2.51 (s, 4 H). ^{13}C NMR (300 MHz, $CDCl_3$): 168.7, 159.0, 158.7, 138.7, 135.6, 135.3, 134.3 134.0, 131.4, 130.9, 130.8, 130.7, 119.9, 112.7, 112.4, 68.3, 31.9, 29.7, 29.6, 29.5, 29.4, 29.3, 29.2, 26.2, 22.7, 14.1. MS (MALDI-TOF): m/z 2544 $[M + H]^+$. HRMS (MALDI-TOF): Calcd. for $C_{172}H_{211}N_{10}O_8$: 2544.6406. Found: 2544.6423.

Compound T3

A solution of compound **1** (16 mg, 0.053 mmol) in formic acid (10 mL) and CH_2Cl_2 (10 mL) was stirred at room temperature

for 12 h and then concentrated with a rotavapor to give the corresponding ethyl ester as a green solid. The ester was added to a solution of porphyrin **3** (62 mg, 0.052 mmol) and DMAP (10 mg) in CH_2Cl_2 (6 mL). After stirring for 20 min, EDCI (0.10 g, 0.52 mmol) was added. The mixture was stirred at room temperature for 14 h and then washed with water (5 mL), saturated sodium bicarbonate solution (5 mL) and brine (5 mL) and dried over sodium sulfate. After the solvent was removed under reduced pressure, the resulting residue was purified by column chromatography on silica gel (CH_2Cl_2–MeOH 100 : 1) to give **T3** as a purple solid (54 mg, 74%). ^{1}H NMR (300 MHz, $CDCl_3$): 8.86–8.84 (m, 8 H), 8.42 (s, 1 H), 8.35 (d, J = 10.5 Hz, 2 H), 8.19 (d, J = 8.4 Hz, 2 H), 8.11–7.97 (m, 10 H), 7.70 (s, 2 H), 7.23–7.16 (m, 6 H), 4.45 (q, J = 6.9 Hz, 2 H), 4.19–4.12 (m, 6 H), 2.00–1.90 (m, 6 H), 1.59–1.55 (m, 6 H), 1.48–1.25 (m, 48 H), 0.95–0.87 (m, 12 H), –2.73 (s, 2 H). ^{13}C NMR (300 MHz, $CDCl_3$): 168.7, 165.0, 159.0, 158.9, 145.6, 142.4, 140.2, 139.4, 138.9, 137.6, 135.6, 135.5, 135.2, 134.4, 134.3, 131.1, 131.0, 121.8, 120.2, 120.1, 120.0, 118.9, 118.4, 112.7, 81.4, 68.3, 32.0, 31.9, 29.8, 29.7, 29.6, 29.5, 29.4, 29.3, 28.4, 26.3, 22.8, 22.7, 14.2. MS (MALDI-TOF): m/z 1409 $[M + H]^+$. HRMS (MALDI-TOF): Calcd. for $C_{94}H_{114}N_5O_6$: 1408.8764. Found: 1408.8760.

Compound T4

To a mixture of compound **4** (11 mg, 0.05 mmol) in toluene (2 mL) and oxalyl dichloride (1 mL) was added a drop of DMF. The mixture was heated under reflux for 4 h and then concentrated under reduced pressure. The resulting residue was dissolved in toluene (10 mL) and the solution added to a stirred solution of porphyrin **3** (120 mg, 0.10 mmol) and pyridine (0.05 mL) in toluene (5 mL). The solution was stirred for 12 h and then successively washed with water (10 mL), saturated sodium bicarbonate solution (10 mL) and brine (50 mL) and dried over sodium sulfate. Upon removal of the solvent, the crude product was subjected to column chromatography (CH_2Cl_2–THF 100 : 1) to give **T4** as a purple solid (78 mg, 61%). ^{1}H NMR (300 MHz, $CDCl_3$-CD_3CN): 8.92–8.88 (m, 16 H), 8.68 (s, 2 H), 8.26–8.25 (m, 6 H), 8.17 (d, J = 7.5 Hz, 2 H), 8.12 (4 H), 8.07 (d, J = 8.7 Hz, 12 H), 7.24 (d, J = 8.7 Hz, 12 H), 4.25–4.21 (m, 12 H), 2.00–1.97 (m, 12 H), 1.63–1.60 (m, 12 H), 1.48–1.26 (m, 96 H), 0.90 (t, J = 6.3 Hz, 18 H), –2.74 (s, 4 H). ^{13}C NMR (300 MHz, $CDCl_3$): 167.8, 158.9, 158.3, 138.7, 137.6, 135.4, 134.9, 134.8, 134.3, 134.0, 133.6, 133.3, 130.9, 129.1, 127.0, 124.4, 120.0, 119.7, 118.9, 112.6, 111.9, 68.2, 67.6, 29.8, 29.7, 29.6, 29.5, 29.4, 29.3, 26.3, 26.2, 22.7, 14.2. MS (MALDI-TOF): m/z 2546 $[M + H]^+$. HRMS (MALDI-TOF): Calcd. for $C_{172}H_{211}N_{10}O_8$: 2544.6406. Found: 2544.6423.

Compound 5

A solution of compound **4** (216 mg, 1.0 mmol) and sulfuric acid (98%, 0.5 mL) in ethanol (40 mL) was heated under reflux for 18 h, cooled to room temperature, neutralized with diluted hydrochloric acid to pH = 5, and then concentrated under reduced pressure. The resulting slurry was extracted with ethyl acetate (80 mM). The organic phase was washed with saturated sodium bicarbonate solution (40 mL), water (40 mL) and brine (40 mL) and dried over sodium sulfate. After the solvent was removed, compound **5** was obtained as a white solid (0.26 g, 95%). ^{1}H NMR (300 MHz, $CDCl_3$): 8.63 (s, 2 H), 8.13 (d, J = 8.7 Hz, 2 H), 8.00 (d, J = 8.7 Hz, 2 H), 4.46 (q, 4 H), 1.46 (t, J = 7.2 Hz, 6 H). MS (EI): m/z 272 $[M]^+$.

Compound 6

A mixture of **5** (0.27 g, 1.00 mmol) and lithium hydroxide monohydrate (42 mg, 1.00 mmol) in THF (15 mL) and water (5 mL) was stirred at room temperature for 2.5 h and neutralized with diluted hydrochloric acid (1 N) to pH = 3. The solution was concentrated under reduced pressure and the resulting slurry was extracted with ethyl acetate (50 mL). After work up, the crude product was recrystallized from ethyl acetate and *n*-hexane to afford **6** as a white solid (0.13 g, 52%). ^{1}H NMR (300 MHz, CD_3COCD_3): 8.72 (d, J = 6.9 Hz, 2 H), 8.23–8.12 (m, 4 H), 4.44 (q, 2 H), 1.43 (t, J = 7.2 Hz, 3 H). MS (EI): m/z 244 $[M]^+$.

Compound T5

To a stirred solution of **6** (13 mg, 0.053 mmol), **3** (62 mg, 0.053 mmol) and DMAP (10 mg) in THF (10 mL) was added EDCI (0.10 g, 0.52 mmol). The mixture was stirred at room temperature for 14 h and concentrated. The resulting slurry was dissolved in CH_2Cl_2 (30 mL) and the solution washed successively with water (30 mL), saturated sodium bicarbonate solution (30 mL), water (30 mL) and brine (30 mL) and dried over sodium sulfate. Upon removal of the solvent under reduced pressure, the resulting residue was purified by column chromatography (CH_2Cl_2) to give compound **T5** as a purple solid (37 mg, 49%). ^{1}H NMR (300 MHz, $CDCl_3$): 8.87 (s, 8 H), 8.68 (s, 1 H), 8.54 (s, 1 H), 8.36 (s, 1 H), 8.24 (d, J = 8.4 Hz, 2 H), 8.12–8.00 (m, 12 H), 7.27–7.22 (m, 6 H), 4.49 (q, 2 H), 4.22–4.19 (m, 6 H), 1.99–1.94 (m, 6 H), 1.63–1.60 (m, 6 H), 1.51–1.25 (m, 48 H), 0.90–0.85 (m, 12 H), –2.74 (s, 2 H). ^{13}C NMR (300 MHz, $CDCl_3$): 167.8, 158.9, 158.3, 138.7, 137.6, 135.6, 135.2, 134.3, 134.0, 133.6, 130.9, 130.3, 129.2, 127.3, 126.4, 124.4, 119.9, 118.4, 112.7, 111.9, 68.3, 31.9, 29.7, 29.6, 29.5, 29.4, 29.3, 26.2, 22.7, 14.4, 14.1. MS (MALDI-TOF): m/z 1409 $[M + H]^+$. HRMS (MALDI-TOF): Calcd. for $C_{94}H_{114}N_5O_6$: 1408.8764. Found: 1408.8781.

Typical process for the gelation test

The tested compound was mixed with 0.1 mL of solvent in a capped test tube of 0.5 cm in diameter. The mixture was heated until the solid was dissolved and then allowed to cool down to 25 °C. After standing for 1 hour, the sample vial was turned upside down. When the suppression of the fluidity of the solvent was observed, it was defined as gelation. For those that formed gel, more solvent was added and the test was repeated until gel was not formed. The concentration obtained for the last test was defined as the lowest gelation concentration.

Acknowledgements

We thank the National Science Foundation of China (Nos. 20732007, 20621062, 20672137, 20872167), the National Basic Research Program (2007CB80801) and Chinese Academy of Sciences (KJCX2-YW-H13) for financial support and Mr Gui-Tao Wang for his assistance.

Notes and references

1 K. M. Kadish, K. M. Smith and R. Guilard, *The Porphyrin Handbook*, Academic, San Diego, 2000, vol. 6.
2 S. J. Lee, J. T. Hupp and S. T. Nguyen, *J. Am. Chem. Soc.*, 2008, **130**, 9632–9633.
3 R. van Hameren, P. Schon, A. M. van Buul, J. Hoogboom, S. V. Lazarenko, J. W. Gerritsen, H. Engelkamp, P. C. M. Christianen, H. A. Heus, J. C. Maan, T. Rasing, S. Speller, A. E. Rowan, J. A. A. W. Elemans and R. J. M. Nolte, *Science*, 2006, **314**, 1433–1436.
4 Z. Wang, K. J. Ho, C. J. Medforth and J. A. Shelnutt, *Adv. Mater.*, 2006, **18**, 2557–2560.
5 Z. Wang, C. J. Medforth and J. A. Shelnutt, *J. Am. Chem. Soc.*, 2004, **126**, 15954–15955.
6 B. Liu, D.-J. Qian, M. Chen, T. Wakayama, C. Nakamura and J. Miyake, *Chem. Commun.*, 2006, 3175–3177.
7 T. Komatsu, M. Moritake and E. Tsuchida, *Chem.–Eur. J.*, 2003, **9**, 4626–4633.
8 Y. Li, X. Li, Y. Li, H. Liu, S. Wang, H. Gang, J. Li, N. Wang, X. He and D. Zhu, *Angew. Chem., Int. Ed.*, 2006, **45**, 3639–3643.
9 M. J. Gunter, S. M. Farquhar and T. P. Jeynes, *Org. Biomol. Chem.*, 2003, **1**, 4097–4112.
10 M. J. Gunter and S. M. Farquhar, *Org. Biomol. Chem.*, 2003, **1**, 3450–3457.
11 K. D. Johnstone, K. Yamaguchi and M. J. Gunter, *Org. Biomol. Chem.*, 2005, **3**, 3008–3017.
12 M. Shirakawa, N. Fujita and S. Shinkai, *J. Am. Chem. Soc.*, 2003, **125**, 9902–9903.
13 V. Kral, S. Pataridis, V. Setnicka, K. Zaruba, M. Urbanova and K. Volka, *Tetrahedron*, 2005, **61**, 5499–5506.
14 T. Kishida, N. Fujita, O. Hirata and S. Shinkai, *Org. Biomol. Chem.*, 2006, **4**, 1902–1909.
15 Y. Li, T. Wang and M. Liu, *Soft Matter*, 2007, **3**, 1312–1317.
16 H. Jintoku, T. Sagawa, T. Sawada, M. Takafuji, H. Hachisako and H. Ihara, *Tetrahedron Lett.*, 2008, **49**, 3987–3990.
17 A. G. Anderson Jr and B. M. Steckler, *J. Am. Chem. Soc.*, 1959, **81**, 4941–4946.
18 M. J. S. Dewar, *The Molecular Orbital Theory of Organic Chemistry*, McGraw-Hill, New York, 1969.
19 S. V. Shevyakov, H. Li, R. Muthyala, A. E. Asato, J. C. Croney, D. M. Jameson and R. S. H. Liu, *J. Phys. Chem. A*, 2003, **107**, 3295–3299.
20 G. Treboux, P. Lapstun and K. Silverbrook, *J. Phys. Chem. B*, 1998, **102**, 8978–8980.
21 P. G. Lacroix, I. Malfant, G. Iftime, A. C. Razus, K. Nakatani and J. A. Delaire, *Chem.–Eur. J.*, 2000, **6**, 2599–2608.
22 S. Ito, H. Inabe, N. Morita, K. Ohta, T. Kitamura and K. Imafuku, *J. Am. Chem. Soc.*, 2003, **125**, 1669–1680.
23 A. Strachota, V. Cimrova and E. Thorn-Csanyi, *Macromol. Symp.*, 2008, **268**, 66–71.
24 F. Wang, Y.-H. Lai and M.-Y. Han, *Macromolecules*, 2004, **37**, 3222–3230.
25 S. Schmitt, M. Baumgarten, J. Simon and K. Hafner, *Angew. Chem., Int. Ed.*, 1998, **37**, 1077–1081.
26 A. F. M. M. Rahman, S. Bhattacharya, X. Peng, T. Kimura and N. Komatsu, *Chem. Commun.*, 2008, 1196–1198.
27 K. Kurotobi and A. Osuka, *Org. Lett.*, 2005, **7**, 1055–1058.
28 E. K. L. Yeow, M. Ziolek, J. Karolczak, S. V. Shevyakov, A. E. Asato, A. Maciejewski and R. P. Steer, *J. Phys. Chem. A*, 2004, **108**, 10980–10988.
29 J. Zindel, S. Maitra and D. A. Lightner, *Synthesis*, 1996, 1217–1222.
30 V. Sol, J. C. Blais, V. Carre, R. Granet, M. Guilloton, M. Spiro and P. Krausz, *J. Org. Chem.*, 1999, **64**, 4431–4444.
31 M. Piacenza and S. Grimme, *J. Am. Chem. Soc.*, 2005, **127**, 14841–14848.
32 Y. Che, A. Datar, K. Balakrishnan and L. Zang, *J. Am. Chem. Soc.*, 2007, **129**, 7234–7235.
33 M. Yang, W. Wang, F. Yuang, X. Zhang, J. Li, F. Liang, B. He, B. Minch and G. Wegner, *J. Am. Chem. Soc.*, 2005, **127**, 15107–15111.
34 A. Ajayaghosh, R. Varghese, V. K. Praveen and S. Mahesh, *Angew. Chem., Int. Ed.*, 2006, **45**, 3261–3264.
35 K. Kano, K. Fukuda, H. Wakami, R. Nishiyabu and R. F. Pasternack, *J. Am. Chem. Soc.*, 2000, **122**, 7494–7502.
36 S. Okada and H. Segawa, *J. Am. Chem. Soc.*, 2003, **125**, 2792–2796.
37 I. Yoshikawa, J. Sawayama and K. Araki, *Angew. Chem., Int. Ed.*, 2008, **47**, 1038–1041.